Study of the molecular geometry of Caramboxin toxin found in star flower (Averrhoa carambola L.)

R. Gobato[1]

Abstract

The present work describes the equilibrium configuration of the caramboxin molecule studied using the Hartree-Fock (HF) and Density functional theory (DFT) calculations. With the DFT calculations, the total energy for the singlet state of caramboxin molecule has been estimated to be -933.3870701 a.u. Furthermore, the binding energy of the caramboxin molecule has been estimated to be 171.636 kJ/mol. The carambola or star fruit is a fruit used for human consumption in juices, desserts, pastries, custards, jellies, or even in natural consumption. Recent research indicates that it has great toxicity for people with kidney failure, and may even lead to death. Experiments demonstrated that it has glutamatergic effects, which means that it affects the function of the neurotransmitter glutamate, thus explaining the neurological effects. Our calculations indicate that the main active sites in carambox are the -OH (alcohols) groups, and the two carboxyl (-COOH) groups.

Keywords

Averrhoa carambola L., B3LYP, Caramboxin, Density Functional Theory (DFT), Hartree-Fock (HF), Molecular Dynamic.

[1] *Secretaria de Estado da Educação do Paraná (SEED/PR), CEJC, Laboratório de Biofísica e Modelagem Molecular, Rua Rocha Pombo, 953, Centro, Bela V. do Paraíso/PR, 86130-000, Brasil.*
Corresponding author: [1]ricardogobato@seed.pr.gov.br

Introduction

An evergreen shrubby vine, *Caramboxin*, carambola (*Averrhoa carambola L.*) fruit is known for its unique star shape and rich golden color. [1] The oxalidaceae family possesses seven genera representing more than two hundred species, which are distributed principally in the tropical and sub-tropical regions of the world. [2] The genus *Averrhoa* contains two species: Bilimbi (*Averrhoa bilimbi L.*) and carambola (*Averrhoa carambola L.*). Carambola is also known as star fruit. It is considered the more important between the two species. The fruit is cultivated extensively in India and China. [2]

The fruit was found to be oblong in shape, being on an average, 7.92 cm long and 5.24 cm in width. The weight of the green mature fruits was significantly different than those of half-ripe and ripe fruits. The pH of the fruit increased with the advance in maturity. Ripe fruits were significantly less acidic (pH 3.44) than green mature (pH 2.40) and half-ripe (pH 2.71) fruits. [1]

Patients suffering from chronic kidney disease are frequently intoxicated after ingesting star fruit. The main symptoms of this intoxication are named in the picture. Bioguided chemical procedures resulted in the discovery of caramboxin, which is a phenylalanine-like molecule that is responsible for intoxication. Functional experiments *in vivo* and *in vitro*

point towards the glutamatergic ionotropic molecular actions of caramboxin, which explains its convulsant and neurodegenerative properties. [1]

Experiments demonstrated that it has glutamatergic effects, which means that it affects the function of the neurotransmitter glutamate, thus explaining the neurological effects. The active and toxic substance was recently discovered and named the Caramboxin, Its chemical structure is similar to the amino acid phenylalanine, core with hydroxy, methoxy, and carboxy additions. [1]

Physicochemical Properties of Caramboxin

Density: 1.5 ± 0.1 g/cm^3
Boiling Point: 494.4 ± 45.0 °C at 760 mmHg
Vapor Pressure: 0.0 ± 1.3 mmHg at 25 °C
Enthalpy of Vaporization: 80.2 ± 3.0 kJ/mol
Flash Point: 252.8 ± 28.7 °C
Index of Refraction: 1.625
Molar Refractivity: 61.0 ± 0.3 cm^3
H bond acceptors: 7
H bond donors: 5
Freely Rotating Bonds: 5
Rule of 5 Violations: 1
Polar Surface Area: 130 $Å^2$
Polarizability: 24.2 ± 0.5 10-24 cm^3
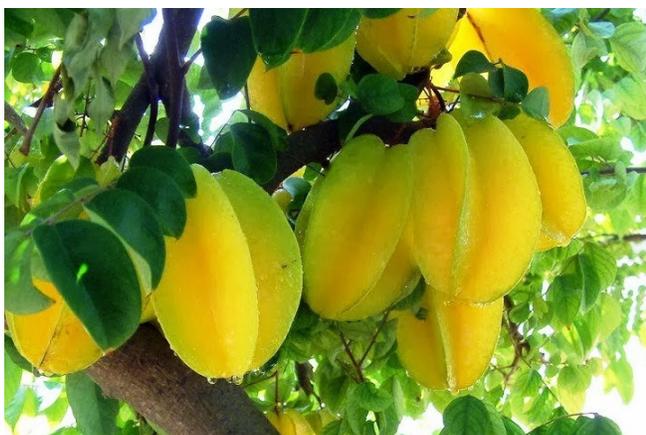
Figure 1. Fruit of carambola (*Averrhoa carambola L.*) [3, 4]

Surface Tension: 74.0 ± 3.0 dyne/cm
Molar Volume: 172.4 ± 3.0 cm^3
Chemical formula: $C_{11}H_{13}NO_6$
Molar mass: 255.23 g·mol^{-1}
Synonyms: 2-Carboxy-3-hydroxy-5-methoxyphenylalanin,
2-Carboxy-3-hydroxy-5-methoxyphenylalanine,
2-Carboxy-3-hydroxy-5-méthoxyphénylalanine,
Caramboxin, Phenylalanine,
2-carboxy-3-hydroxy-5-methoxy-
[5]

One of the fruits most commonly used to decorate the dishes, especially during the year-end parties, carambola can be fatal for patients with chronic kidney disease (CKD), regardless of the amount ingested. Therefore, members of Bauru Support and Assistance Renal Chronic Association (Abrec) and the Diabetic Association of Bauru (ADB) took the opportunity to launch a warning to the population. [6]

The seemingly innocent fruit can lead people with kidney failure to death, because it contains a neurotoxin that can not be filtered by the kidneys with a problem. "Therefore, patients with renal failure from different levels can not eat carambola, is juice, jam, fruit, tea, finally, any derivative product" strengthens nephrologist Tereza Maria Speranza Faifer. [6]

If there is fruit intake, symptoms ranging from persistent hiccups to seizures (see illustration above) and may lead to death. Relative to the amount considered fatal of carambola, the nephrologist unaware of a study in this area. "Therefore, I do the ban to all my patients with any type of kidney failure. Prevention is better than cure ", argues the doctor. [6]

1. Materials and Methods

A cluster of 6 computer models was used: Prescott-256 Celeron D processors, featuring double the L1 cache (16 KB) and L2 cache (256 KB), Socket 478 clock speeds of 2.13 GHz; Memory DDR2 PC4200 512MB; Hitachi HDS728080PLAT20 80 GB and CD-R.

Principles Calculations

The first principles calculations have been performed to study the equilibrium configuration of caramboxin molecule using the *Hyperchem 7.5 Evaluation* [7], *Molden* a general molecular and electronic structure processing program [8], *Avogadro*: an advanced semantic chemical editor, visualization, and analysis platform [9] and *GAMESS* is a computational chemistry software program and stands for General Atomic and Molecular Electronic Structure System [10]. set of programs. The first principles approaches can be classified into two main categories: the Hartree-Fock approach and the density functional approach. [11] In what follows, we briefly consider the Hartree-Fock method and the density functional theory.

The Hartree-Fock self–consistent method is based on the one-electron approximation in which the motion of each electron in the effective field of all the other electrons is governed by a one-particle Schrödinger equation. The Hartree-Fock approximation takes into account of the correlation arising due to the electrons of the same spin, however, the motion of the electrons of the opposite spin remains uncorrelated in this approximation. The methods beyond self-consistent field methods, which treat the phenomenon associated with the many-electron system properly, are known as the electron correlation methods. One of the approaches to electron correlation is the Møller-Plesset (MP) perturbation theory in which the Hartree-Fock energy is improved by obtaining a perturbation expansion for the correlation energy. [12] However, MP calculations are not variational and can produce an energy value below the true energy. [13]

Another first principles approach to calculate the electronic structure for many-electron systems is the density functional theory (DFT). In this theory, the exchange-correlation energy is expressed, at least formally, as a functional of the resulting electron density distribution, and the electronic states are solved for self-consistently as in the Hartree-Fock approximation. [11, 14, 15, 16] The density functional theory is, in principle, exact but, in practice, both exchange and dynamic correlation effects are treated approximately. [17]

Method
A hybrid exchange-correlation functional is usually constructed as a linear combination of the Hartree–Fock exact exchange functional,

$$E_x^{HF} =$$

$$= -\frac{1}{2}\sum_{i,j}\int\int \psi_i^*(\mathbf{r_1})\psi_j^*(\mathbf{r_1})\frac{1}{r_{12}}\psi_i(\mathbf{r_2})\psi_j(\mathbf{r_2})d\mathbf{r_1}d\mathbf{r_2}, \quad (1)$$

and any number of exchange and correlation explicit density functionals. The parameters determining the weight of

each individual functional are typically specified by fitting the functional's predictions to experimental or accurately calculated thermochemical data, although in the case of the "adiabatic connection functionals" the weights can be set a priori. [18]

B3LYP

The B3LYP (Becke, three-parameter, Lee-Yang-Parr) [19, 20] exchange-correlation functional is:

$$E_{xc}^{B3LYP} = E_x^{LDA} + a_0(E_x^{HF} - E_x^{LDA}) +$$

$$+ a_x(E_x^{GGA} - E_x^{LDA}) + E_c^{LDA} + a_c(E_c^{GGA} - E_c^{LDA}) \quad (2)$$

where as an example

$a_0 = 0.20$; $a_x = 0.72$; $a_x = 0.72$; $a_c = 0.81$; $a_c = 0.81$; E_x^{GGA} and E_x^{GGA} and are generalized gradient approximations: the Becke 88 exchange functional [21] and the correlation functional of Lee, Yang and Parr [22] for B3LYP, and E_c^{DA} is the VWN local-density approximation to the correlation functional. [23]

The three parameters defining B3LYP have been taken without modification from Becke's original fitting of the analogous B3PW91 functional to a set of atomization energies, ionization potentials, proton affinities, and total atomic energies. [24]

The first principles methods (i.e. HF and DFT) discussed above can be implemented with the aid of the *GAMESS* set of programs to study the electronic structure and to determine the various physical properties of many-electron systems. [10] A basis set is the mathematical description of the orbitals within a system (which in turn combine to approximate the total electronic wavefunction) used to perform the theoretical calculation. [25] 3-21G, 3-21G*, 6-31G, 6-31G*, 6-31G**, 6-311G, 6-311G*, 6-311G** are the basis sets used in the calculations. The functional Becke-style one parameter functional using modified Perdew-Wang exchange and Perdew-Wang 91 correlation is used for DFT Calculations. [17, 26]

Molecular dynamics

The great computational speed of molecular mechanics allows for its use in procedures such as molecular dynamics, conformational energy searching, and docking. All the procedures require large numbers of energy evaluations. Molecular mechanics methods are based on the following principles: Nuclei and electrons are lumped into atom-like particles; Atom-like particles are spherical (radii obtained from measurements or theory) and have a net charge (obtained from theory); Interactions are based on springs and classical potentials; Interactions must be preassigned to specific sets of atoms; Interactions determine the spatial distribution of atom-like particles and their energies;

Note how these principles differ from those of quantum mechanics. [13, 27, 28, 29, 30, 31]

In short the goal of molecular mechanics is to predict the detailed structure and physical properties of molecules. Examples of physical properties that can be calculated include enthalpies of formation, entropies, dipole moments, and strain energies. Molecular mechanics calculates the energy of a molecule and then adjusts the energy through changes in bond lengths and angles to obtain the minimum energy structure. [28, 29, 30, 31, 13]

Steric Energy

A molecule can possess different kinds of energy such as bond and thermal energy. Molecular mechanics calculates the steric energy of a molecule–the energy due to the geometry or conformation of a molecule. Energy is minimized in nature, and the conformation of a molecule that is favored is the lowest energy conformation. Knowledge of the conformation of a molecule is important because the structure of a molecule often has a great effect on its reactivity. The effect of structure on reactivity is important for large molecules like proteins. Studies of the conformation of proteins are difficult and therefore interesting, because their size makes many different conformations possible.

$$E_{se} = E_{str} + E_{bend} + E_{str-bend} + E_{oop} + E_{tor} + E_{VdW} + E_{qq} \quad (3)$$

The steric energy, bond stretching, bending, stretch-bend, out of plane, and torsion interactions are called bonded interactions because the atoms involved must be directly bonded or bonded to a common atom. The Van der Waals and electrostatic (qq) interactions are between non-bonded atoms.[28, 29, 30, 31, 32, 33].

The dynamic was held in Molecular Mechanics Force Field (Mm+), Eq. (3), after the quantum computation using the functional B3LYP [34] and base 6-311G** [10]. The molecular dynamics at algorithm Polak-Ribiere [35], conjugate gradient, at the termination condition: RMS gradient [36] of 0,1 kcal/A.mol or 405 maximum cycles in vacuum. Molecular properties: electrostatic potential 3D mapped isosurface, mapped function range, minimum -0.087 at maximum $+0.699$, display range legend, from positive color red to negative color blue, Electrostatic Potential contour value of 0.05, gourand shaded surface. [31, 33, 37]

Table 1. Dipole moment (field-independent basis, Debye)

X = 4.3825	Y = 1.0314	Z = 2.4340	Tot = 5.1181

Table 2. Quadrupole moment (field-independent basis, Debye-Ang)

XX = -117.4906	YY = -103.6384	ZZ = -104.3173
XY= -25.2050	XZ = -5.3379	YZ = -5.0598

Table 3. Traceless Quadrupole moment (field-independent basis, Debye-Ang

XX = -9.0085	YY = 4.8437	ZZ = 4.1648
XY = -25.2050	XZ = -5.3379	YZ = -5.0598

2. Discussions and Conclusions

In Figure (1) one has a photograph of several fruits of the carambola in its tree. The fruits are in the greenish yellow color already time of being harvested, that is, mature.

Figures (2) and (3) have four images of the molecular structure of caramboxin, which symmetric in with a 180 degree rotation in the plane of the page, and three of them rendering Gouraud shaded surface, both of Figures (2) and (3).

In Figures (2) and (3) four images of the molecular structure of caramboxin are shown from the top down. These in a snapshot after an optimization geometry of its molecular structure, departed from the structure of the obtained chemspider, Table (4), to the final structure, obtained through the molecular simulation in the functional B3LYP and base 6-31G ** and a molecular dynamics Mm + , Table (5). The top one has a graphical molecular plot of its electrostatic potential, in 3D Mapped Isosurface, from blue (negative potential) to red (positive potential).

The second top-down graphical molecular plot of its electrostatic potential, in Isosurface 3D, in dark blue color, a strong negative bond potential of oxygen atoms, prone to hydrogen bonding, with atoms of its own molecule, and / Or with other molecules.

The third top-down graphic plot a molecular of its electrostatic potential, in 2D Contours, that is, a cut in the 3D structure of the molecule. Likewise, in the dark blue color, a strong negative bond potential of Oxygen atoms, prone to hydrogen bonding with other molecules, and / or with atoms of their own molecule.

The fourth from top to bottom, that is, the first from bottom to top, a molecular graphic plot of the final molecular structure at the base and base 6-31G **, obtained in Molden, showing the hydrogen of the oxygen atom number 14, terminal Alcohol, making hydrogen bond, with the atom of Oxygen number 18. Likewise the number 22 hydrogen atom of the amine group, making a hydrogen bond (hydrogen bond) with Oxygen number 17, of the terminal alcohol.

In Figure (5) we have the electrostatic potential of the molecular structure of caramboxin rendering Jorgensen-Salem. [7, 10]

Tables (1), (2) and (3) present the results of the Dipole moment, Quadrupole moment, Traceless Quadrupole moment. [10]

We used the bases 3-21G, 3-21G*, 6-31G, 6-31G*, 6-31G**, 6-311G, 6-311G*, 6-311G** are the basis sets used in the calculations, but here we present only the results of 6-311G**.

Our calculations indicate that the main active sites in carambox are the -OH (alcohols) groups, and the two carboxyl groups.

Acknowledgements

References

[1] N. Narain; P. S. Bora; H. J. Holschuh and M. A. da S. Vasconcelos. Physical and chemical composition of carambola fruit (averrhoa carambola l.) at three stages of maturity. *Cienc. Tecnol. Aliment.*, 3(3):144–148, 2001.

[2] W. B. Hayes. *Fruit Growing in India*. Kitabistan, Allahabad., 1960.

[3] Os 16 benefícios da carambola para saúde. Dicas de Saúde, September, 28 2016.

[4] A carambola e seus benefícios!!!!!!, 2016 September, 28.

[5] Caramboxin. ChemSpider Search and share chemistry, 2015. ChemSpider ID32779488.

[6] C. Milanez. Entidades fazem um alerta para perigo da carambola. Jornal da Cidade, September 2016.

[7] Hypercube. Hyperchem.7.5 evaluation, 2003. http://www.hyper.com/.

[8] G. Schaftenaar and J. H. Noordik. Molden: a pre- and post-processing program for molecular and electronic structures. *J. Comput. -Aided Mol. Design*, 14:123–134, September 2000.

[9] M. D. Hanwell; D. E. Curtis; D. C. Lonie; T. Vandermeersch; E. Zurek and G. R. Hutchison. Avogadro: an advanced semantic chemical editor, visualization, and analysis platform. *J Cheminform*, 17(4), August 13 2012.

[10] T .L. Windus; M. Dupuis M. W. Schmidt; K. K. .Baldridge; J. A. Boatz; S. T. Elbert; M. S. Gordon; J. H. Jensen; S. Koseki; N. Matsunaga; K .A. Nguyen; S. Su and J. A. Montgomery. General atomic and molecular electronic structure system. *J. Comput. Chem.*, 14:1347–1363, 1993.

[11] K. Ohno; K. Esfarjani and Y. Kawazoe. *Computational Material Science*. Springer-Verlag, Berlin, 1999.

[12] A. Szabo and N.S.Ostlund. *Modern Quantum Chemistry*. Dover Publications, New York, 1989.

[13] I.N. Levine. *Quantum Chemistry*. Pearson Education (Singapore) Pte. Ltd., Indian Branch, 482 F. I. E. Patparganj, Delhi 110 092, India, 5th ed edition, 2003.

[14] K. Wolfram and M. C. Hothausen. *Introduction to DFT for Chemists*. John Wiley & Sons, Inc. New York, 2nd ed edition, 2001.

[15] P. Hohenberg and W. Kohn. Inhomogeneous electron gas. *Phys. Rev.*, (136):B864–B871, 1964.

[16] W. Kohn and L. J. Sham. Self-consistent equations including exchange and correlation effects. *Phys. Rev.*, (140):A1133, 1965.

[17] J. M. Thijssen. *Computational Physics*. Cambridge University Press, Cambridge, 2001.

[18] J. P. Perdew; M. Ernzerhof and K. Burke. Rationale for mixing exact exchange with density functional approximations. *J. Chem. Phys*, 105(22):9982–9985, 1996.

[19] K. Kim and K. D. Jordan. Comparison of Density Functional and MP2 Calculations on the Water Monomer and Dimer. *J. Phys. Chem.*, 40(98):10089–10094, 1994.

[20] P.J. Stephens; F. J. Devlin; C. F. Chabalowski and M. J. Frisch. Ab Initio Calculation of Vibrational Absorption and Circular Dichroism Spectra Using Density Functional Force Fields. *J. Phys. Chem.*, 45(98):11623–11627, 1994.

[21] A. D. Becke. Density-functional exchange-energy approximation with correct asymptotic behavior. *Phys. Rev. A.*, 38(6):3098–3100, 1988.

[22] C. Lee; W. Yang and R. G. Parr. Development of the Colle-Salvetti correlation-energy formula into a functional of the electron density. *Phys. Rev. B*, 37(2):785–789, 1988.

[23] S. H. Vosko; L. Wilk and M. Nusair. Accurate spin-dependent electron liquid correlation energies for local spin density calculations: a critical analysis. *Can. J. Phys*, 58(8):1200–1211, 1980.

[24] A. D. Becke. Density-functional thermochemistry III. The role of exact exchang. *J. Chem. Phys.*, 98(7):5648–5652, 1993.

[25] J.B. Foresman and Æleen Frisch. *Exploring Chemistry with Electronic Structure Methods*. Gaussian, Inc. Pittsburgh, PA, 2nd ed edition, 1996.

[26] L. Mainali; D. R. Mishra and M. M. Aryal. First principles calculations to study the equilibrium configuration of ozone molecule. Department of Biophysics. Medical College of Wisconsin. 8701 Watertown Plank Road. Milwaukee, WI 53226.

[27] E. Eliav. *Elementary introduction to Molecular Mechanics and Dynamics*, Jun 2013.

[28] Thomas W. Shattuck. *Colby College Molecular Mechanics Tutorial*. Department of Chemistry, Colby College, Waterville, Maine 04901., September 2008.

[29] W. D. Cornell; P. Cieplak; C. I.Bayly; I. R. Gould; K. M. Merz Jr.; D. M. Ferguson; D. C. Spellmeyer; T. Fox; J. W. Caldwell and P. A. Kollman. A second generation force field for the simulation of proteins, nucleic acids, and organic molecules. *J. Am. Chem. Soc.*, 117:5179–5197, 1995.

[30] W. J. Hehre. *A Guide to Molecular Mechanics and Quantum Chemical Calculations, Wavefunction*. Inc., Irvine, CA, 2003.

[31] R. Gobato; D. F. G. Fedrigo and A. Gobato. Molecular geometry of alkaloids present in seeds of mexican prickly poppy. *Cornell University Library. Quantitative Biology. Other Quantitative Biology*, 15 Jul 2015. arXiv:1507.05042.

[32] R. Gobato. Benzocaína, um estudo computacional. Master's thesis, Universidade Estadual de Londrina (UEL), 2008.

[33] R. Gobato; A. Gobato and D. F. G. Fedrigo. Molecular electrostatic potential of the main monoterpenoids compounds found in oil lemon tahiti - (citrus latifolia var tahiti). *Parana Journal of Science and Education*, 1(1):1–10, November 2015.

[34] W. Yang C. Lee and R.G. Parr. *Phys. Rev. B*, 37:785–789, 1988.

[35] E. Polak. *Computational Methods in Optimization*, volume 77. Elsevier, 111 Fifth Avenue, New York, New York 10003, 1971.

[36] Anthony K. Rappé and Carla J. Casewit. *Molecular Mechanics Across Chemistry*. University Science Books, 55D Gate Five Road, Sausalito, CA 94965, 1952(1997).

[37] R. Gobato; D. F. G. Fedrigo and A. Gobato. Allocryptopine, berberine, chelerythrine, copsitine, dihydrosanguinarine, protopine and sanguinarine. molecular geometry of the main alkaloids found in the seeds of argemone mexicana linn. *Parana Journal of Science and Education*, 1(2):7–16, December 2015.

3. Figures
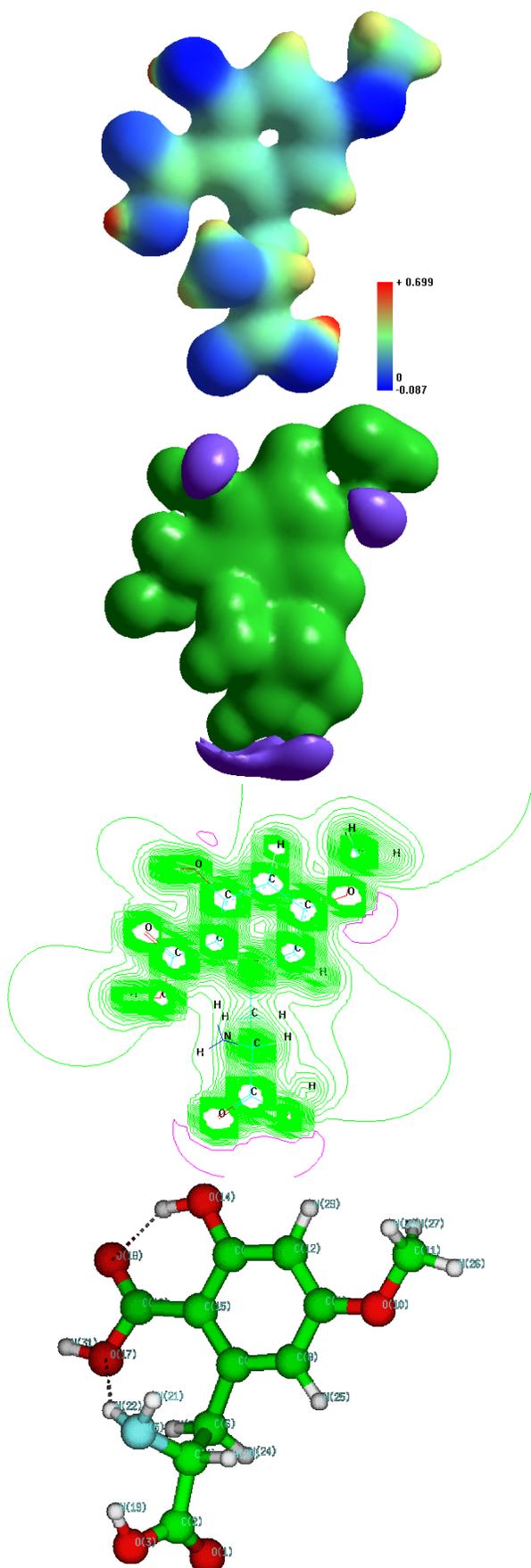
Figure 2. From bottom to top we have: a molecular structure of the caramboxin rod model; Electrostatic potential 2D contours, Electrostatic potential 3D Isosurface and Electrostatic potential isosurfaces 3D Mapped Isosurface) [7, 8, 9, 10]
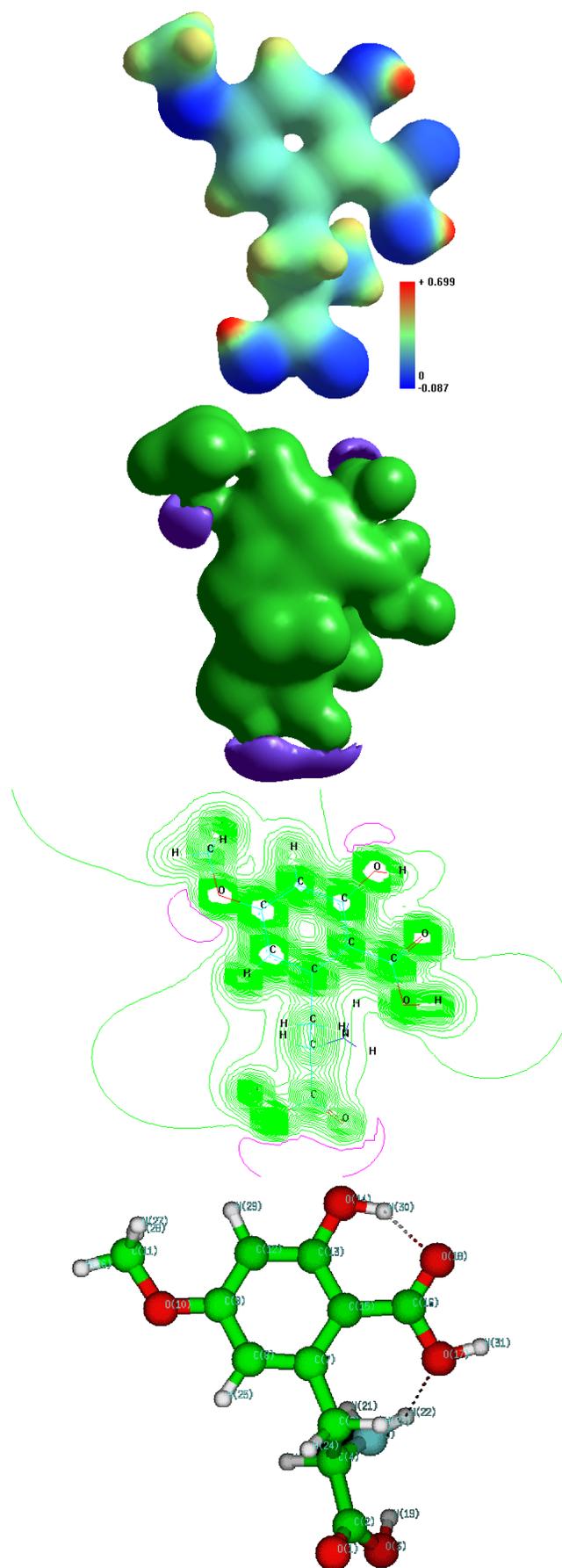
Figure 3. This figure is symmetrical to Figure (2) with 180 degrees of rotation. [7, 8, 9, 10]
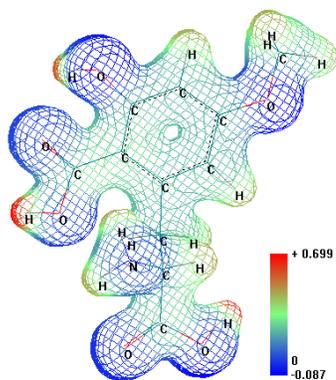
Figure 4. Here we have the electrostatic potential of the molecular structure of caramboxin rendering Jorgensen-Salem. [7, 8, 9, 10]

Attachments

Table 4. File Caramboxin.pdb - ChemSpider Search and Share Chemistry [5]

HETATM	1	O		1	-0.983	-5.387	0.107
HETATM	2	C		2	-0.191	-5.540	-0.808
HETATM	3	O		3	-0.485	-6.390	-1.828
HETATM	4	C		4	1.125	-4.780	-0.808
HETATM	5	N		5	1.896	-5.135	-2.008
HETATM	6	C		6	1.933	-5.152	0.450
HETATM	7	C		7	3.249	-4.392	0.450
HETATM	8	C		8	3.249	-3.052	0.450
HETATM	9	C		9	4.514	-2.322	0.450
HETATM	10	O		10	4.514	-0.962	0.450
HETATM	11	C		11	5.862	-0.485	0.450
HETATM	12	C		12	5.674	-2.992	0.450
HETATM	13	C		13	5.674	-4.452	0.450
HETATM	14	O		14	6.852	-5.132	0.450
HETATM	15	C		15	4.514	-5.122	0.450
HETATM	16	C		16	4.514	-6.582	0.450
HETATM	17	O		17	3.336	-7.262	0.450
HETATM	18	O		18	5.570	-7.192	0.450
CONECT	1	2					
CONECT	2	1	3	4			
CONECT	3	2					
CONECT	4	2	5	6			
CONECT	5	4					
CONECT	6	4	7				
CONECT	7	6	8	15			
CONECT	8	7	9				
CONECT	9	8	10	12			
CONECT	10	9	11				
CONECT	11	10					
CONECT	12	9	13				
CONECT	13	12	14	15			
CONECT	14	13					
CONECT	15	7	13	16			
CONECT	16	15	17	18			
CONECT	17	16					
CONECT	18	16					
CONECT	3	3					
CONECT	6	4					
CONECT	4	5					
CONECT	4	5					
CONECT	5	6					
CONECT	5	6					
CONECT	3	8					
CONECT	4	11					
CONECT	4	11					
CONECT	4	11					
CONECT	1	12					
CONECT	8	14					
CONECT	8	17					
END							

Table 5. File Caramboxin.pdb. (.pdb output after an optimization geometry on B3LYP/6-311G**) [8, 7]

HEADER							
HETATM	1	O	2	2	-0.981	-4.953	0.141
HETATM	2	C	2	2	-0.298	-5.320	-0.779
HETATM	3	O	2	2	-0.764	-6.050	-1.798
HETATM	4	C	2	2	1.201	-4.960	-0.917
HETATM	5	N	2	2	1.806	-5.792	-1.970
HETATM	6	C	2	2	1.884	-4.999	0.468
HETATM	7	C	2	2	3.293	-4.432	0.456
HETATM	8	C	2	2	3.378	-3.054	0.510
HETATM	9	C	2	2	4.614	-2.384	0.510
HETATM	10	O	2	2	4.543	-1.036	0.558
HETATM	11	C	2	2	5.755	-0.284	0.585
HETATM	12	C	2	2	5.796	-3.108	0.477
HETATM	13	C	2	2	5.748	-4.505	0.441
HETATM	14	O	2	2	6.933	-5.124	0.437
HETATM	15	C	2	2	4.499	-5.204	0.402
HETATM	16	C	2	2	4.589	-6.661	0.334
HETATM	17	O	2	2	3.436	-7.355	0.150
HETATM	18	O	2	2	5.635	-7.302	0.411
HETATM	19	H	2	2	0.025	-6.214	-2.365
HETATM	20	H	2	2	1.209	-3.924	-1.273
HETATM	21	H	2	2	2.492	-5.275	-2.506
HETATM	22	H	2	2	2.275	-6.595	-1.562
HETATM	23	H	2	2	1.854	-6.013	0.857
HETATM	24	H	2	2	1.270	-4.388	1.132
HETATM	25	H	2	2	2.481	-2.451	0.576
HETATM	26	H	2	2	5.451	0.760	0.623
HETATM	27	H	2	2	6.350	-0.525	1.471
HETATM	28	H	2	2	6.349	-0.459	-0.317
HETATM	29	H	2	2	6.772	-2.647	0.496
HETATM	30	H	2	2	6.763	-6.095	0.449
HETATM	31	H	2	2	3.694	-8.290	0.166